Compensating the Impact of Residual Energy on Time Domain Dielectric Response using Time-Varying Model

Chandra Madhab Banerjee, Deepak Mishra, *Sr. Member IEEE,* Arijit Baral, *Sr. Member, IEEE* and Sivaji Chakravorti, *Sr. Member IEEE*

***Abstract*— Analysis of polarization and depolarization current is a widely accepted method for diagnosing power transformer insulation. The accuracy of such techniques depends significantly on the premise that measurement of insulation response has been done correctly. During field measurement, equipment sometimes fails to record proper current, even after applying DC charging voltage. In such cases, the polarization current profile gets affected by residual energy. Recently, a Conventional Debye Model (CDM) based approach has been reported to solve the issue. The CDM-based approach relies on identifying the correct time-invariant branch parameters, by minimizing the deviation between measured and estimated value of several performance parameters, through an iterative technique. This coupled with presence of multiple branches in CDM makes the overall method time consuming and computationally intensive. The paper proposes a non-iterative methodology, based on a model with time-varying parameters that is capable of achieving the same result. This not only saves time but also reduces overall data post processing and computation burden required for diagnosis. Performance of the proposed method is tested on data obtained from the oil-paper sample and several real-life power transformers. The proposed method is observed to be capable of estimating paper-moisture (using affected data) with more than 95% accuracy for in-service units. The time required for achieving this is found to be approximately 1/3rd of that required by CDM-based technique (which could provide result with maximum 90% accuracy).**

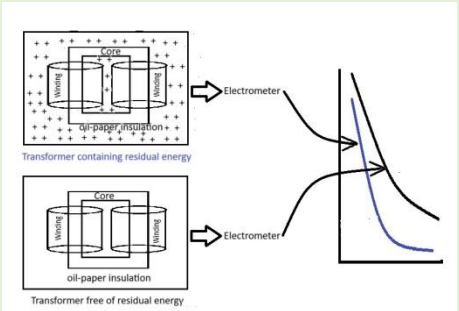

***Index Terms*— Polarization and depolarization current, Electrometer, Residual Energy, Power Transformer**

I. Introduction

IN modern power systems, the power transformer plays a significant role. To ensure uninterrupted operation, it should have a good healthy condition. Various non-invasive insulation tests are conducted to ensure good condition of the transformer's insulation [1-5]. One example of such tests is polarization and depolarization current measurement (PDC) [3, 6-8]. To measure proper PDC, measuring instruments must be properly connected [7-8]. Various literatures have reported different condition-monitoring techniques based on PDC data [7-8]. Such analysis becomes effective only when the measured data is recorded correctly. As per the information provided by the utility, during the measurement of PDC data from an in-service transformer, in quite a few cases, the Electrometer could not measure any data even though the charging voltage was applied across the insulation. Later in the paper, it is explained that under certain circumstances, the insulation may continue to get charged during this phase. This issue, primarily caused by improper connection, results in unwanted energy input to the insulation before PDC measurement. In the present work, this unwanted energy injected into the insulation is termed "Residual energy". Charges introduced by residual energy can be removed if the terminals of the power transformer are kept short-circuited with the ground for a sufficiently long duration after the issue is detected and rectified. As such connection issues are generally detected and after that rectified within a very short time (spanning a few 100 seconds), the utility operators often ignore the effect of residual energy. Hence, the measured polarization current gets affected by the residual energy. Analysis of such affected polarization current cannot be expected to provide a satisfactory diagnosis. Here, a methodology is proposed to remove the effect of residual energy from the affected polarization current for reliable condition monitoring of the power transformer.

The motivation of the paper is to have an effective and reliable diagnosis within a short duration of time using a cost-

Chandra Madhab Banerjee is with the Philips, India (e-mail: cmbanerjee90@gmail.com).

Deepak Mishra is with the Department of Electrical Engineering, Indian Maritime University, India (e-mail: dmishra@imu.ac.in)

Arijit Baral is with the Department of Electrical Engineering, IIT (ISM) Dhanbad, Dhanbad 826004, India (e-mail:a_baral@ieee.org)

Sivaji Chakravorti is with the with the Department of Electrical Engineering, Jadavpur University, Kolkata 700032, India (e-mail: s_chakrav@yahoo.com)

effective system. It is understood that costly commercial equipment like IDAX or DIRANA cannot be deployed in large scale. On the other hand, Electrometer based setup is much less capital intensive and hence can be deployed at a larger number. Further, literature [14] shows that the entire polarization current can be predicted using data recorded for 10 min. It is known fact that IDAX or DIRANA takes much longer time to operate [15-16]. Further it is shown in [11] that Time Varying Model (TVM) can be used to predict *%pm* which is close to that estimated by IDAX. However, employing TVM [11] and forecasting based methodology [14] necessitates measurement of insulation response from a charge-free insulation. As the presence of residual energy does not alter the monotonically decreasing nature of polarization current, its presence may result in inaccurate estimation of *%pm* using TVM based methodology. Hence, compensation for residual energy is necessary for carrying out an effective diagnosis.

The rest of this paper is organized as follows. Section II briefly describes the Electrometer-based PDC measurement setup. This section also describes the limitations of the previously reported methodology to solve the residual energy-related problem. Section III briefly describes the TVM formulation followed by its advantage over existing time-invariant model. Section IV presents a TVM-based methodology to address the residual-energy related issue effectively. Section V and VI describe the application and validation of the proposed methodology using data recorded from sample and real-life transformers. The power ratings of the transformers used in the present work are tabulated in Table 1.

TABLE 1: POWER RATING OF THE TESTED TRANSFORMERS

Transformer Name	Power Rating	Operational Age
Trafo-1	167 MVA, 220 kV	12
Trafo-2	240MVA,220kV	14

II. EFFECT OF RESIDUAL ENERGY ON PDC

The present work uses a KEITHLEY 6517B Electrometer-based setup to measure PDC data (schematic shown in Fig. 1) [6, 9]. PDC measurement is a non-intrusive offline method. Prior to measurement, both windings are initially short-circuited and allowed to remain in this state long enough to eliminate any residual charge. Following this, the two terminals of each winding is shorted. Thus, forming two terminals across which a DC excitation voltage is applied to facilitate polarization current measurement. A typical charging voltage of 1000 V is utilized for this process [7]. Given the low magnitude of the resulting relaxation current, an Electrometer is generally used to ensure precise data acquisition. A LabVIEW script is employed to generate control instructions and facilitate data acquisition. These commands are sent to the controller module (CM) through a USB-GPIB converter. The CM interacts with multiple components to regulate data collection and processing. Its key roles include:

1. Configuring the voltage source of the Electrometer by sending appropriate commands.
2. Adjusting the current sensing module of the Electrometer through control instructions.
3. Engaging the LV Contactor Module to connect the Electrometer's Te_3 terminals with the LV terminal during PDC measurement.
4. Activating the HV Contactor Module to link the HV terminal of the insulation to Te_1 (or ground) during polarization and depolarization current measurement.
5. Relaying the data collected by the metering module back to the computer.
6. Operating the LV and HV Contactor Modules to short the LV and HV terminals as needed.

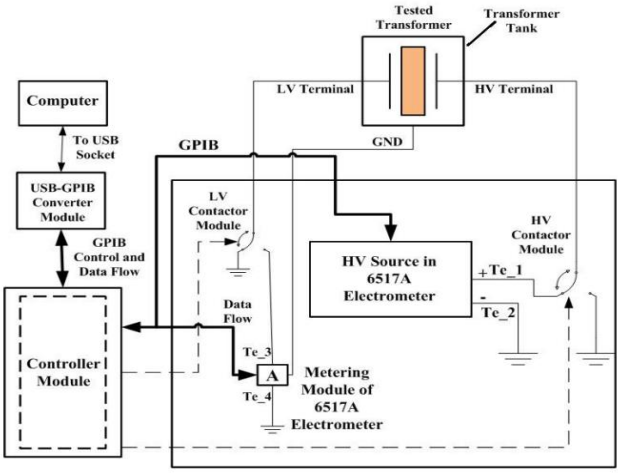

Fig. 1. Set up to measure polarization current.

A feedback ammeter module deployed inside the Electrometer is used to sense the current signal [19]. Fig. 2 depicts the block diagram of the feedback ammeter module. High gain Op-Amp with feedback module restricts the voltage burden of Thevenin's equivalent of the concerned current source to a few hundred μV [19]. This facilitates measurement of low amplitude currents. The block-diagram of the setup is shown in Fig.3. It can be observed from Fig. 3 that if either of the BLACK or RED wire is not properly attached to the insulation, the Electrometer will be unable to record data. In case the Black wire is not properly connected, the dc charging voltage applied to the insulation using RED wire will introduce dipole energy during this phase. Furthermore, it is observed that a loose connection between the tank and the Electrometer's GND terminal can introduce noise, rendering the recorded data useless. During this time, the charging voltage may continue to charge the insulation thus increasing its dipolar energy content. Due to the involvement of human operators, this kind of error cannot always be avoided. Furthermore, the setup shown in Fig. 1 does not possess the capability to check whether all the connections are made properly or not. During the PDC measurement, the Electrometer is not allowed to measure the

polarization current for a few seconds to avoid transients. This further makes it difficult for the operator to detect about possible improper connections. For handling high frequency noise, an in-build median filter is used in the Electrometer-based hardware [17]. Using such filtering technique, noise-free PDC data have been measured at many sites located throughout India with satisfactory accuracy [6, 9]. However, such a filtering technique cannot remove low-frequency noise.

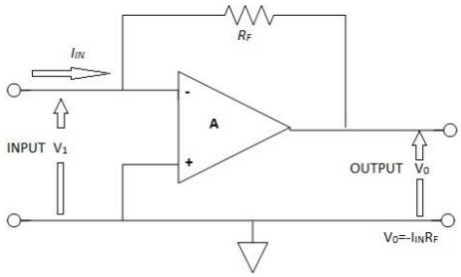

Fig.2. Typical Block diagram of a feedback ammeter [19]

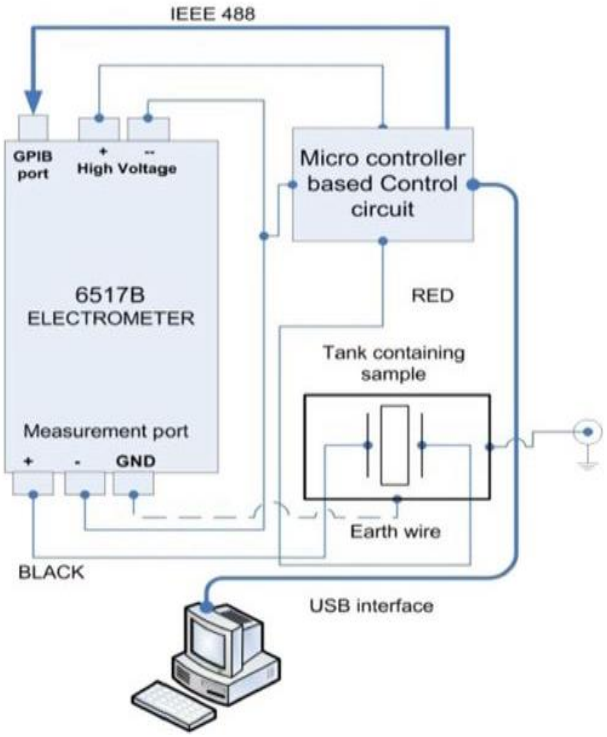

Fig. 3. Schematic Circuit Diagram of 6517B Electrometer [10].

Utilities generally assume that the small-time duration for which inaccurate data is recorded does not influence the relaxation of the dipole, which has a significantly large time constant [7]. It is understood that the presence of residual energy implies that the insulation will not be entirely charge-free before PDC measurement. As far as an insulation model is concerned, the presence of residual energy will manifest itself as a voltage (V_p) across the insulation. A CDM-based iterative technique to solve this issue is reported in [10]. Though effective, the time-consuming iterative method is computationally intensive and requires data which in turn need to be measured using different instrument. In order to improve readability and emphasize the advantage provided by the proposed technique, the reported method is briefly explained below. In CDM, the polarization current is approximated as a weighted sum of n exponential functions given in (1).

$$ip(t) = \sum_{j=1}^{n} M_j \, exp(-t/\tau_j) \quad (1)$$

In (1), M_j and $1/\tau_j$ represent the amplitude and decay rate of the i^{th} exponential function, respectively. Each of the exponential decay function mentioned in (1) is represented as a RC branch in CDM. The time-invariant resistive (R_j) and capacitive (C_j) element representing the j^{th} branch is related to M_j and τ_j using (2)

$$R_j = \frac{V}{M_j} \;\; ; \;\; C_j = \frac{\tau_j}{R_j} \quad (2)$$

In [10], the effect of V_p has been effectively modelled by assuming the presence of voltage source V_j in the j^{th} branch of the CDM as illustrated in Fig. 4. Once the value of V_j is identified, correct values of R_j & C_j can be identified.

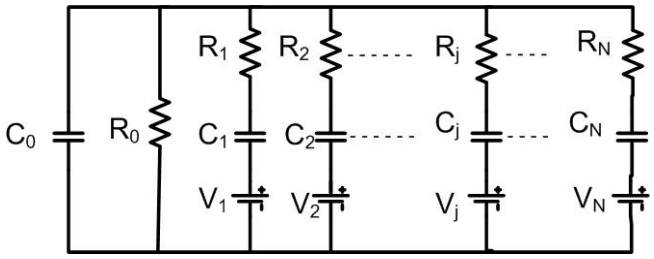

Fig. 4. Structural Modifications in CDM due to Residual Energy

The expression of initial estimate $V_j[1]$ is shown in Fig. 4 is modeled by (3). In equation (3), $R_j[1]$, $C_j[1]$ represent the initial value of resistive and capacitive element in j^{th} branch, respectively. On the other hand, V and $t_{apply}[1]$correspond to the applied DC charging voltage and the initial estimate of the period during which the Electrometer was unable to capture data.

$$V_j[1] = V \times \left(1 - \exp\left(-\frac{t_{apply}[1]}{R_j[1] \times C_j[1]}\right)\right) \quad (3)$$

Due to the nature of the issue and the polarity of the DC charging voltage, V_j inherently opposes the applied step voltage. Consequently, when Vp is present, the insulation model yields a value of R_j that is lower than the actual value. However, the impact of V_p is less significant in branches with larger time constants. It should be noted that R_j alone is insufficient for assessing cellulose insulation condition, as it is influenced by insulation geometry. Instead, performance parameters such as Transfer Function Zero (Z_1), known for its reduced sensitivity to insulation geometry, can be used for this purpose [8]. The preceding discussion indicates that an accurate diagnosis is possible once t_{apply} in (3) is determined. The CDM-based methodology accomplishes this through an iterative process that estimates t_{apply} by comparing predicted and observed values of several parameters. In the k^{th} iteration, with $k > 1$, the error between computed and measured values for the following parameters are evaluated:

- Dielectric Absorption Ratio (DAR)
- Polarization Index (PI)

- Insulation Resistance (IR) at 60s
- tanδ

These errors, each normalized by their corresponding measured values, are used to obtain the total error E_r. Subsequently, parameters, $R_j[k], C_j[k]$ and $t_{apply}[k]$ are derived using (4).

$$\left.\begin{aligned} R_j[k] &= R_j[k-1]\times\left(1+\frac{V_j[k-1]}{V}\right)\\ C_j[k] &= \tau_j[k-1]/R_j[k]\\ \tau_j[k] &= R_j[k]\times C_j[k] \end{aligned}\right\} \quad (4)$$

The dependency of the factor $V_j(k-1)$ in (4) on the values from the $(k-1)^{th}$ iteration is established in Equation (5).

$$V_j[k-1] = V\times\left(1-\exp\left(-\frac{t_{apply}[k-1]}{\tau_j[k-1]}\right)\right) \quad (5)$$

The iteration procedure begins with the initial values $R_j[k=1]$ and $C_j[k=1]$ obtained from the CDM, parameterized using the affected polarization current. The initial value of t_{apply} (1) is set to a small predetermined number. Upon completing the k^{th} iteration, t_{conn} is recalculated using (6).

$$t_{apply}[k] = t_{apply}[k-1]/Er \quad (6)$$

The proposed method utilizes IR measured at 60s, primarily because it is commonly accessible to utilities. However, it is flexible enough to accommodate any data points from the Insulation Resistance Profile (IRP) [18]. The iterative branch parameter adjustment halts when further changes no longer significantly influence the total error *Er*. The above-mentioned method is summarized in the form of algorithm given below [10]

Step 1. Obtain CDM parameters using measured data.
Step 2. Assume $t_{apply} \rightarrow 0$.
Step 3. Evaluate V_i using i^{th} branch parameters of CDM and present value of t_{apply}.
Step 4. Update i^{th} branch parameters of CDM using obtained value of V_j (Step 3) and measured data
Step 5. Calculate *tanδ*, Insulation Resistance (IR), Polarization Index (PI), Dielectric Absorption Ratio (DAR) using CDM parameters obtained in Step4.
Step 6. Obtain total error (*Er*) using deviation between measured and calculated values of *tanδ, IR, PI, DAR*.
Step 7. If *Er* is greater than predetermined small value, update t_{apply} value based on *Er* and go to Step3.
Step 8. Predict the nature of compensated polarization current using latest CDM parameters

At present, a methodology is yet to be reported that can identify the optimum number of CDM branches corresponding to a given response. As per available literature, any number of branches are acceptable as long as the fitting accuracy is maintained to a high value. It is understood that considering a large number of CDM branches indeed lead to better fitting of the insulation response. However, the iterative methodology coupled with a high number of branches will lead to high computation time. Later in the paper, it is shown that the time taken and the number of iteration required for finding t_{apply} are indeed dependent on the number of CDM branches. In the present paper, a less time-consuming, reliable method based on TVM having a unique structure is proposed to compensate the effect of residual energy. In order to improve readability, section III first describes the formulation methodology of TVM [11] and thereafter the TVM-based methodology is detailed.

III. Time-Varying Model: A Brief Theory

When polarization current $i_p(t)$ measurement is conducted, the dipoles in the oil-paper insulation begin aligning with the applied electric field. This reorientation generates a current within the insulation, referred to as the relaxation current $i_{relax}(t)$. The flow of this current causes an increase in the stored charge *Q(t)* within the dielectric. As the dipoles continue to align, an opposing electric field develops, eventually balancing the applied field. This balance results in the relaxation current $i_{relax}(t)$ gradually reducing to zero, leaving only a minimal DC leakage current I_{dc}. The connection between insulation impedance and stored charge is illustrated by (7) through (9).

$$Z(t) = \frac{V}{i_p(t)} \quad (7)$$

$$C(t) = \frac{Q(t)}{V} \quad (8)$$

$$Q(t) = \int_0^t i_{relax}(t)dt\,;\; i_p(t) = i_{relax} + I_{dc} \quad (9)$$

In (7), *Z(t)* signifies the impedance contributed by the series combination of time-dependent *R(t)* and *C(t)*. As more dipoles reorient, the resistance *R(t)* increases. At longer time intervals, $i_{relax}(t)$ tends toward zero as $i_p(t)$ becomes asymptotic to the time axis. At this stage, Z(t) attains a steady-state value equal to the DC resistance R_0. The dielectric response in TVM is modeled by considering dipole relaxation to exhibit a pure Debye characteristic [11]. Thus, the relaxation phenomenon is mathematically represented by an exponential decay function, as outlined in (10).

$$i_p(t) = A\times\exp\left(-\frac{t}{\tau}\right) \quad (10)$$

Where A signifies the amplitude and τ is the time constant associated with the relaxation function. The present paper uses the branch parameter of TVM to obtain compensated polarization current profile. In order to improve readability,

the formulation of TVM (shown in Fig. 5) is re-iterated below. A window function having unity magnitude and a specific time span ($t_{WF}=t_1<t<t_2$) is multiplied with the polarization current $i_p(t)$ to obtain $i_{WF}(t)$ (shown in (11)).

$$i_{WF}(t) = i_p(t) \times \left[u(t-t_1) - u(t-t_2) \right] \tag{11}$$

In (11), t_1 represents the instant the current $i_p(t)$ measurement starts. Next, $i_{WF}(t)$ obtained through (11) is curve fitted with an exponential decay function shown in (12).

$$i_{WF}(t) = A_{WF} \times \exp\left(-t / \tau_{WF}\right) \tag{12}$$

Thereafter, information obtained from (12) are used to obtain resistance ($R(t)$) and capacitance ($C(t)$) for the time duration considered using (13)[11].

$$\left.\begin{aligned} R(t) &= \frac{V}{A_{WF}} \\ C(t) &= \frac{\tau_{WF}}{R_{WF}} \end{aligned}\right\} \; for\; t_1 < t < t_2 \tag{13}$$

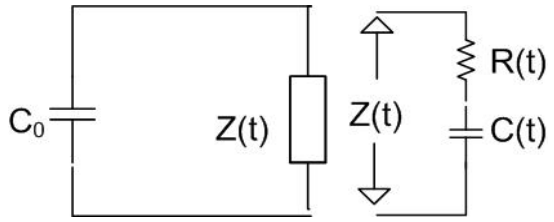

Fig. 5. Structure of Time-Varying Model.

Next, the window function is shifted to the right so that it occupies a new time span $t_{WF}=t_3<t<t_4$ such that $t_1<t_3<t_2$ and $t_2<t_4$. The resistance and capacitance values for this time span are then determined using (12) and (13). This process is repeated until the window function reaches the end of the polarization current. In order to better understand the key differences between CDM and TVM, the two models are compared in the Table 2.

TABLE 2: DIFFERENCE BETWEEN CDM AND TVM

Sl.No.	Properties	CDM	TVM
1	Number of Branches	Not Fixed. Depends on curve fitting parameters. Usually greater than 8 for in-service transformers.	Two. One containing C_0 and the other $Z(t)$
2	Model formulation	Tries to model response of different type of dipoles present separately.	Models the overall response of all dipoles present through $Z(t)$.
3	Branch Parameters	Constant, Time-invariant	Time-dependent profile of $Z(t)$.
4	Uniqueness of branch parameters	Not unique. Parameter values vary with number of branches	Fixed number of branches. R(t), C(t) profiles are unique
5	Estimated aging-sensitive parameter	Depends on number of branches and parameters therein.	Depends on R(t) profile.
6	Accuracy of model-based diagnosis technique	Varies for a given insulation response as parameters are not unique	For a given insulation response is constant

IV. PROPOSED METHODOLOGY

In TVM, the value of resistance, $R(t)$ and capacitance, $C(t)$ model the resultant dipole response corresponding to a particular time instant t. Henceforth, residual unaffected and affected polarization current will be denoted as i_p and i_{paf} respectively. The parameter of TVM corresponding to i_{paf} will have the influence of residual energy. If the polarization current is influenced by residual energy, it is necessary to short circuit the terminals of the windings for a significant duration. The stored energy will be neutralized during this short-circuiting phase. After this short-circuiting phase gets over, an Insulation Tester (here, Fluke 1550B) needs to be used to measure insulation impedance ($Z_m(t)$) profile. It is worth mentioning here that insulation impedance ($Z_m(t)$) (measured by Insulation Tester) corresponding to different time instant is obtained by simply dividing the applied voltage (Vm) across insulation and measured current (Im) at different instant. The $Z_m(t)$ profile is mainly influenced by time-varying resistance and capacitance as insulation is resistive-capacitive in nature [1,11-12]. The insulation impedance measured by Insulation Tester is used to obtain the TVM parameter R^P_{WF} of the insulation using (14). On the other hand, the TVM corresponding to i_{paf} provides resistance, $R(t)$-value at any time instant [11]. If the system is unaffected by its initial dipole energy, then the resistance value obtained using TVM and Insulation Tester (using (14)) should match at the tested time instant.

$$\left.\begin{aligned} \mathrm{Im}(t) &= \frac{Vm}{Z_m(t)}; t = t_1 \; to \; t_2 \\ Im(t) &= A^P_{WF} \times \exp\left(-t / \tau^P_{WF}\right) \; for\; t = t_1 \; to \; t_2 \\ R^P_{WF}(t_1) &= \frac{Vm}{A^P_{WF}} \end{aligned}\right\} \tag{14}$$

Due to the influence of residual energy, there will be a mismatch between the insulation's resistance values (obtained using TVM and Insulation Tester). Hence, the difference (r_{diff}) between the resistance values (obtained using TVM and Insulation Tester) is calculated using (15).

$$r_{diff}(t_1) = R^P_{WF}(t_1) - R(t_1) \tag{15}$$

The resistance, r_{diff} opposes the flow of polarization current, i_{paf}. It can be understood that the magnitude of residual voltage, V_p of the insulation, is equal to the product of $r_{diff}(t_1)$ and $I_m(t_1)$ given by (16).

$$V_p = I_m(t_1) \times r_{diff}(t_1) \tag{16}$$

The current (i_{ref}) corresponding to this residual voltage is the difference between i_p and i_{paf}. The i_{ref} is calculated using V_p given by (17).

$$i_{ref}(t) = \frac{V_p \times \exp\left(-\frac{t}{R(t)\times C(t)}\right)}{R(t)} \tag{17}$$

The mathematical expression of the estimated i_p is shown in (18).

$$Estimated\ profile\ of\ ip = i_{paf} + i_{ref} \tag{18}$$

It can be understood from (18) that the proposed TVM-based methodology solves the residual energy related issue in a straight forward manner. Prediction of i_p through (18) is not dependent on minimization of any error (like *Er* in (4)) through iterative adjustment of several branch parameters. Unique branch parameters of TVM facilitates in achieving the correct i_p profile by executing (15) through (18) only once. On the other hand, executing (4) through (6) repeatedly does not always guarantee optimum result as the number of CDM branches and the parameters present therein are not unique. Consequently, it can be understood that the computation involved in executing (18) is significantly less that that is involved for the CDM-based methodology. A detailed performance comparison, in terms of accuracy and running time, between the proposed and available CDM-based methodology is presented later in the paper.

V. APPLICATION TO LABORATORY SAMPLE

Testing the proposed procedure on laboratory samples is essential to determine its efficacy. The steps outlined in [12] are used to build laboratory samples with various amounts of paper moisture. Further, the polarization current was measured from the constructed oil-paper sample under thermal equilibrium conditions. It is understood that measurement temperature, in addition to *%pm*, may also affect the also influence the accuracy of the proposed methodology. Hence, the impact of varying measurement temperature on the performance of the proposed TVM-based methodology has also been studied. To emulate the situation depicted in section II, polarization current was measured from the samples under two different situations (*Situation1* and *Situation2*) using setup shown in Fig. 1 and 3.

In *Situation1*, the constructed samples were intentionally charged for a time duration t_{apply} (to emulate the situation when the Electrometer could not record any current). Thereafter, residual energy affected polarization current, i_{paf} was measured at different temperatures. In *Situation2*, the terminals of the samples were kept short circuited with ground for a prolonged period and no dc voltage was applied prior to PDC measurement. The polarization current, i_p under residual charge free conditions was thereafter measured at different temperatures. In both the cases, the samples were kept within a hot air oven. The oven was used to maintain the thermal equilibrium of the samples at a specific temperature and hence control the measurement temperature.

It is observed that the profile of residual charge affected polarization current (shown in Fig. 6) of sample maintains monotonically decreasing profile. However, its magnitude decreases. It is not possible for a system to have two significantly different polarization current profiles unless significant aging happens within a short time. This suggests that the presence of residual energy reduces the magnitude of the polarization current. Table 3 shows the effectiveness of the suggested methodology on data measured from test samples for different values of measurement temperature and t_{apply}. It can be observed from Table 3 that the correlation coefficient Γ between the measured and estimated profile of i_p is greater than 0.98. Figure 6 shows that the estimated (i_p) polarization current profile, obtained from the uncompensated (i_{paf}) polarization current profile, is almost overlapping with the measured residual charge unaffected polarization current (i_p) of Sample 1.

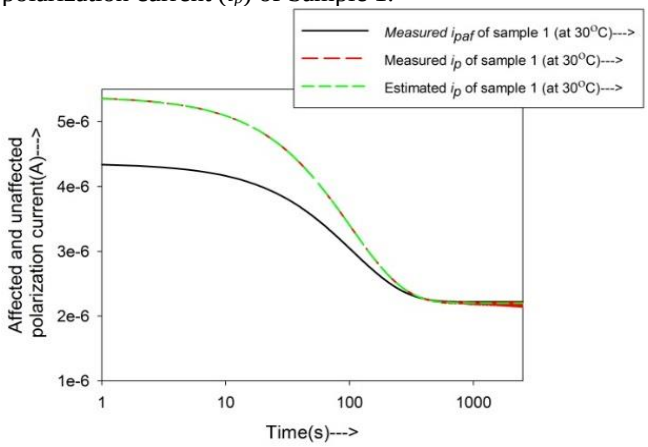

Such a high value of Γ indicates that the proposed methodology can estimate the profile of i_p from the profile of i_{paf} for oil-paper sample. It is known that polarization current can be used to estimate various performance parameters like Paper-moisture (*%pm*) [13], Polarization Index (*PI*) [12]. In the case of laboratory sample, the *%pm* estimation starts by modeling the time varying capacitance *C(t)* profile of TVM using (19).

$$C(t) = \alpha_0 + \gamma \exp(\beta \times t) \tag{19}$$

The parameter β of (19) is reported to be sensitive to *%pm* [13]. Thereafter, the value of *%pm* of a given laboratory sample can be calculated using (20) [13].

$$\%pm = 17.3825 + 3.0965 \times \ln(\beta) \tag{20}$$

Both *%pm* and *PI* are obtained from the measured profile of i_{paf} and the estimated profile of i_p. The percentage error between the measured *%pm* (obtained using IDAX) and that obtained from the measured profile of i_{paf} and i_p is denoted as *%error1* and *%error2* in Table 3, respectively. High value of *%error1*, shown in Table 3 suggests that the analysis based on the profile, i_{paf} will provide inaccurate information about the insulation condition.

TABLE 3: THE IMPACT OF TEMPERATURE (°C) and t_{apply} ON THE EFFECTIVENESS OF THE SUGGESTED METHODOLOGY FOR OIL-PAPER SAMPLES TO PREDICT *%pm*

Sample Name	Temperature (°C)	t_{apply}(s)	%pm (Measured using IDAX)	The correlation coefficient between measured and estimated profile of i_p	Estimated *%pm* from the estimated profile of i_{paf}	*%error1* (in %)	Estimated %pm from the estimated profile of i_p	*%error2* (in %)
Sample 1	30	60	0.6	0.995	0.91	51.66	0.65	8.33
	40	90	0.7	0.983	1.2	71.42	0.76	8.57
	50	120	0.9	0.989	0.4	55.55	0.91	1.11
	60	150	0.9	0.991	0.7	22.22	0.96	6.66
Sample 2	30	60	1.5	0.985	1.1	26.66	1.42	5.33
	40	90	1.7	0.986	1.12	34.11	1.64	3.52
	50	120	1.8	0.994	1.23	31.66	1.73	3.88
	60	150	2.0	0.982	1.34	33.00	1.94	3.00
Sample 3	30	60	1.8	0.984	0.98	45.55	1.64	8.88
	40	90	1.9	0.985	1.2	36.84	1.91	0.52
	50	120	2.1	0.994	1.35	35.71	1.99	5.23
	60	150	2.3	0.996	1.45	36.95	2.12	7.82
Sample 4	30	60	2.2	0.987	1.49	32.27	2.13	3.18
	40	90	2.4	0.984	1.46	39.16	2.21	7.91
	50	120	2.5	0.989	1.74	30.40	2.34	6.40
	60	150	2.7	0.991	1.87	30.74	2.62	2.96
Sample 5	30	60	2.5	0.994	1.37	45.20	2.34	6.40
	40	90	2.7	0.984	1.84	31.85	2.62	2.96
	50	120	2.8	0.983	1.98	29.28	2.66	5.00
	60	150	2.9	0.985	1.96	32.41	2.71	6.55
Sample 6	30	60	3.0	0.982	1.84	38.66	2.74	8.66
	40	90	3.1	0.996	2.12	31.61	2.84	8.38
	50	120	3.2	0.982	2.14	33.12	3.16	1.25
	60	150	3.5	0.981	2.47	29.42	3.39	3.14

TABLE 4: THE IMPACT OF TEMPERATURE (°C) AND t_{apply} ON THE EFFECTIVENESS OF THE SUGGESTED METHODOLOGY FOR OIL-PAPER SAMPLE TO PREDICT *PI*

Sample Name	Temperature (°C)	t_{apply}(s)	%pm (Measured using IDAX)	Measured PI obtained from i_P	Calculated PI from i_{paf}	*%error3* (in %)	Calculated PI from the estimated profile of i_p	*%error4* (in %)
Sample 1	30	60	0.6	1.26	1.96	55	1.25	0.07
	40	90	0.7	1.38	1.72	24	1.40	1.41
	50	120	0.9	1.38	2.2	59	1.40	1.41
	60	150	0.9	1.38	1.66	20	1.40	1.41
Sample 2	30	60	1.5	1.28	1.51	17.6	1.29	0.07
	40	90	1.7	1.21	1.40	15.7	1.23	1.62
	50	120	1.8	1.21	1.40	15.7	1.23	1.61
	60	150	2.0	1.19	1.38	15.6	1.20	0.08
Sample 3	30	60	1.8	1.09	1.33	22.0	1.12	2.02
	40	90	1.9	1.09	1.28	17.4	1.12	2.02
	50	120	2.1	1.06	1.26	15.8	1.07	0.09
	60	150	2.3	1.05	1.28	21.9	1.07	0.09
Sample 4	30	60	2.2	1.11	0.92	16.3	1.10	0.23
	40	90	2.4	1.11	0.92	16.3	1.10	0.61
	50	120	2.5	1.13	0.93	17.07	1.12	0.87
	60	150	2.7	1.14	0.97	14.38	1.13	0.78
Sample 5	30	60	2.5	1.32	1.07	18.33	1.31	0.53
	40	90	2.7	1.34	1.14	14.47	1.33	0.47
	50	120	2.8	1.33	1.12	15.26	1.32	0.6
	60	150	2.9	1.36	1.15	15.14	1.35	0.14
Sample 6	30	60	3.0	1.42	1.19	15.63	1.40	0.83
	40	90	3.1	1.42	1.20	14.92	1.40	0.92
	50	120	3.2	1.46	1.29	11.36	1.44	0.86
	60	150	3.5	1.48	1.29	12.7	1.45	1.7

Hence, the effect of residual energy from the profile of i_{paf} should be removed for reliable analysis of oil-paper insulation. It can be observed from column 9 of Table 3 that the %percentage error (*%error2*) between measured and estimated *%pm* is low. It is worth mentioning here that IDAX/DIRANA accurately measures data from any given insulation. As a result, the authors used IDAX result for validation purposes. The authors agree that DIRANA measure both PDC and FDS simultaneously. DIRANA converts measured time domain dielectric response (polarization current) into frequency domain response (corresponding to low frequency) to reduce measurement time. On the other hand, IDAX employs multi-frequency excitation for obtaining FDS data. Nevertheless DIRANA/IDAX takes approximately 40 minutes measurement time [15-16]. TVM can be used to predict *%pm* which is close to that estimated by IDAX at much lesser time, provided that the response is measured from a charge-free insulation. This makes it advantageous for the utilities to use the TVM coupled PDC based approach for insulation diagnosis. In Table 3, the authors have compared the result between estimated *%pm* (shown in column 8) obtained using the hardware shown in (4) and IDAX data (shown in column 4).

Polarization current of a unit can be used to estimate various performance parameter like, DP value, de-trapped charge, paper conductivity [6, 11, 18].Furthermore, Electrometer-based hardware setup is significantly less expensive than DIRANA/IDAX. The estimated profile of i_p ,obtained using the proposed method from i_{paf} is also utilized to obtain the value of the polarization index (*PI*) for each sample. It can be observed from Table 4 that the percentage error (*%error4*) between the measured and estimated value of PI is low. Hence, it can be opined that the proposed method can neutralize the effect of residual energy from i_{paf} for reliable analysis of oil-paper samples. Before the proposed method can be accepted, it is important to investigate its performance using data collected from real-life in-service transformers. Results corresponding to such analysis are presented in the next section.

VI. APPLICATION ON REAL LIFE TRANSFORMER

Utilities always try to keep power transformers in shutdown condition for as little time as possible. On the other hand, PDC measurement is always performed offline under thermal equilibrium conditions. This suggests that adequate post-shutdown cooling must be given before PDC measurement. Extending the shutdown period in the current scenario is not practically advantageous by performing the second round of measurement after confirming appropriate connections. To ensure complete neutralization of residual energy, a transformer must be kept in the shutdown condition for a prolonged period before the second measurement round. As a result, correcting the affected current, i_{paf}, rather than returning to numerous measurements, is helpful from a practical standpoint for utilities. Hence, the proposed methodology is applied to polarization current data with residual energy issues. The standard deviation (*s.d.*) of time varying resistance profile can be satisfactorily used for estimation of *%pm* using (21) [11].

$$\%\,pm = -7.5841 + 2.9722 \times \ln(100 \times s.d.) \qquad (21)$$

As per literature [11], estimated value of *%pm* maintains good correlation with result obtained from commercial equipment like IDAX. However, it is prerequisite to have residual charge unaffected polarization current corresponding to a transformer for proper functioning of such methodology.

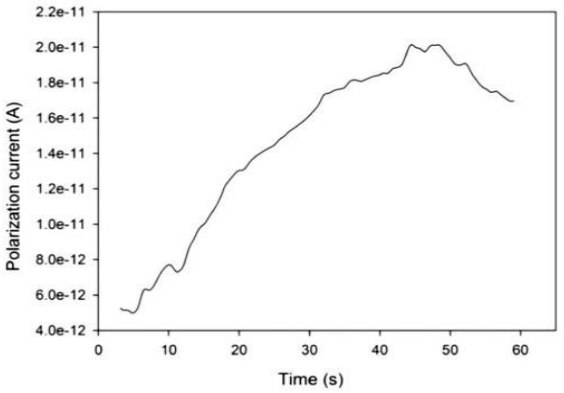

Fig.7.Measured polarization current from Trafo-1 [10]

TABLE 5: THE IMPACT OF TEMPERATURE (°C) AND t_{apply} ON THE EFFECTIVENESS OF THE SUGGESTED METHODOLOGY FOR Trafo-1 AND Trafo-2 TO PREDICT *%pm*

Transformer Name	*%pm* (Measured using IDAX)	Estimated *%pm* from the estimated profile of i_{paf}	*%error1* (in %)	Estimated *%pm* from the estimated profile of i_p	*%error2* (in %)
Trafo-1	0.6	0.37	38.3	0.58	3.3
Trafo-2	2.3	1.1	52.1	2.21	3.9

TABLE 6: THE IMPACT OF TEMPERATURE (°C) AND t_{apply} ON THE EFFECTIVENESS OF THE SUGGESTED METHODOLOGY FOR Trafo-1 AND Trafo-2 TO PREDICT *PI*

Transformer Name	Measured PI obtained from i_p	Calculated PI from i_{paf}	*%error3* (in %)	Calculated PI from the estimated profile of i_p	*%error4* (in %)
Trafo-1	4.6	2.9	36.9	4.7	2.1
Trafo-2	2.3	1.2	47.8	2.24	2.6

Section IV shows that if the profile of i_p is correctly estimated, the performance parameters obtained using commercial equipment will match those obtained using the i_p profile. In the case of Trafo-1, the initially measured polarization current is observed to not have the monotonic decreasing profile (shown in Fig. 7). In the case of Trafo-2, the DAQ system could not record any data. However, 1000V was applied across the terminals of the transformer for nearly 20 seconds. The polarization currents of these units were subsequently measured after ensuring proper connection. However, it is understood that such polarization current were affected by residual energy. To illustrate this fact, *%pm* is estimated using measured residual charge affected polarization current using the methodology depicted in [11]. It can be seen from Table 5 and 6 that the measured and estimated value of both performance parameters, (*%pm* and *PI*) of Trafo-1 and Trafo-2 differs significantly from those obtained using commercial equipment. Thereafter, the proposed method is applied to the residual charge-affected polarization current. Compensated and uncompensated profiles of the polarization current of Trafo1 and Trafo-2 are shown in Fig. 8 and Fig. 9, respectively.

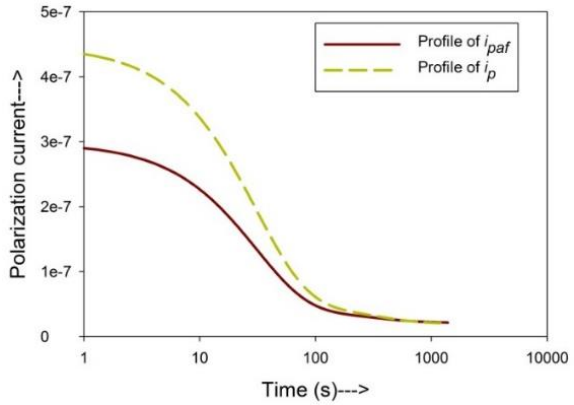

Fig. 8. Compensated (i_p) and uncompensated (i_{paf}) profile of polarization current of Trafo1

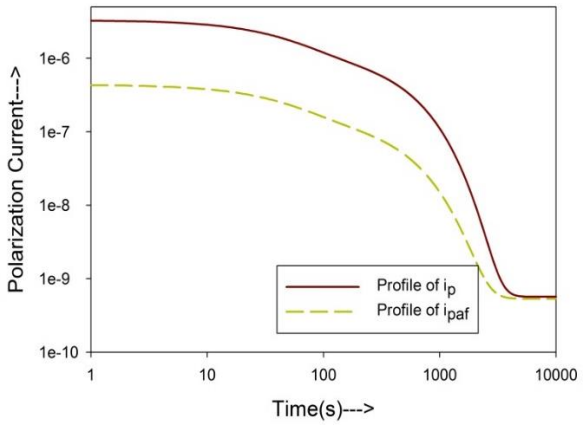

Fig 9. Compensated (i_p) and uncompensated (i_{paf}) profile of polarization current of Trafo2

Again the estimated profile of i_p is used to predict of *%pm* of both the units using the methodology reported in [11]. It can be observed from column 6 of Table 5 that the deviation between estimated (using estimated i_p) and measured *%pm* (*%error2*) is negligible. It can be further observed from column 6 of Table 6 that the percentage error (*%error4*) between the measured and estimated value of PI is also negligible. This result again indicates that the proposed method is capable of compensating for the effect of residual voltage from the affected polarization current of real-life unit.

At this point it is advisable to illustrate the advantage of using TVM in the place of CDM. The performance of the proposed TVM-based methodology is compared with that of reported CDM-based methodology. The comparison is done w.r.t the number of iteration and the overall time for addressing the issue mentioned in the paper. The result of such comparison is tabulated in Table 7.

TABLE 7: COMPARATIVE PERFORMANCE STUDY OF PROPOSED AND TRADITIONAL MODELS

Model type	No of branches	No of iteration	Overall running time (s)	% Error in estimating %pm
Trafo-1				
CDM	9	197	20.36	22.11
	10	207	21.40	20.35
	13	217	22.43	15.31
	15	241	24.91	10.83
	16	245	25.32	10.79
TVM	1	1*	7.76	3.31
Trafo-2				
CDM	8	198	20.47	19.60
	10	209	21.60	16.54
	13	204	21.09	14.16
	14	221	22.84	14.34
TVM	1	1*	8.15	3.92
Sample 4				
CDM	6	208	21.50	13.10
	8	214	22.12	12.57
	10	217	22.43	12.36
	12	219	22.64	10.11
TVM	1	1*	5.85	3.18
Sample 6				
CDM	6	203	20.98	18.33
	8	194	20.05	17.35
	10	206	21.29	19.45
	12	219	22.64	10.61
TVM	1	1*	5.36	3.14

* *The proposed method is non-iterative in nature*

Table 7 show that use of TVM-based methodology leads to better accuracy in estimating %pm (using affected polarization current). Further, use of the proposed methodology leads to less computation and overall less post-processing time of recorded data.

As per the information provided by the utility, the PDC data were measured from Trafo-1 and Trfo-2 at a measurement temperature of $29 \pm 1^{\circ}$C and $31 \pm 1^{\circ}$C, respectively. It is worth mentioning here that the transformer operator have managed to record the polarization current from *Trafo1* for a second time recently at a similar temperature. During the second measurement, no issue related to residual energy was observed by the operator. This provided an additional opportunity to validate the proposed methodology. The measured polarization current is compared with the predicted

data (obtained using the proposed TVM-based approach and residual energy affected data). The correlation coefficients between the measured and predicted profile is observed to be above 0.96. This fact coupled with the data provided in Table 7 makes it evident that the TVM-based technique is indeed capable of predicting correct current profile in less time.

The TVM-based methodology is inherently adaptable due to its data-driven parameter estimation approach. Unlike conventional models that rely on fixed relaxation time constants, TVM extracts time-dependent resistance *R(t)* and *C(t)* parameters dynamically from the recorded polarization and depolarization current (PDC) data. This enables the model to automatically adjust to variations in transformer power ratings, operational age, environmental conditions, and insulation material properties. Since TVM does not require a predefined set of relaxation parameters but rather extracts real-time dielectric behavior, it is scalable to transformers of varying sizes and aging conditions without requiring manual reconfiguration.

To validate the adaptability of TVM, the methodology has been tested on both laboratory oil-paper samples and real-life in-service transformers. In laboratory testing, TVM was applied to samples with different moisture levels and temperatures, demonstrating its ability to capture insulation variations under controlled conditions. For field testing, the method was implemented on multiple transformers with different power ratings and operational ages, and despite variations in residual energy levels, the TVM-based approach is observed to be capable of consistently finding the corrected polarization current profiles (confirmed by the last column of Table 7). This confirms its robustness across transformer types and its ability to neutralize the effects of residual energy effectively. Moreover, TVM-based methodology and (20) are found to be capable of providing results that are in good agreement with those obtained using commercial diagnostic systems such as IDAX and DIRANA, ensuring its adaptability to various testing setups.

One of the primary motivations behind the proposed TVM-based technique has been to provide a cost-effective, reliable, and efficient alternative for transformer insulation diagnostics. Given that IDAX and DIRANA are expensive and time-intensive, utilities can deploy TVM-based analysis more widely due to its lower computational requirements. By eliminating the need for iterative optimization and incorporating real-time parameter adaptation, TVM significantly reduces the cost and computational burden while maintaining high accuracy. This makes it a practical and scalable solution for large-scale implementation in power system maintenance and monitoring. Though the proposed method effectively addresses the issue of residual energy without resorting to an iterative technique, implementation of the proposed method does come with a few challenges mentioned below:

- Requirement of long-duration offline measurement: The proposed method is capable of rectifying the effect of residual energy on measured insulation response, provided that the entire span of measured data, obtained through offline technique, is available.

- The proposed method is not capable of distinguishing the influence of residual energy from any other low-frequency signals that may affect the insulation response. The proposed method would still extract the meaningful insulation response from the affected current. However, it will discard any information that could have been obtained from the low-frequency signal.

- The proposed method assumes that the equipment under testing has undergone sufficient cooling time and the error in data is not due to the effect of temperature transients. Inadequate cooling time or measurement of data during temperature variation may affect the accuracy of the proposed technique.

- The proposed technique further assumes that the charging voltage used during testing of in-service equipment is 1000V. It is reported in literature [3,7] that increase in charging voltage beyond 1000V introduces nonlinearity in response which may not be the influence of residual energy.

VII. CONCLUSIONS

The following conclusions can be drawn based on the findings reported in this article.

1. The proposed method can compensate for residual energy's effect on a real-life transformer's recorded polarization current.
2. The proposed technique enables accurate prediction of current; facilitating the estimation of aging-sensitive parameters. This approach offers a reliable, fast, and convenient method for insulation diagnosis.
3. The present method is a less time-consuming and non-iterative technique.
4. The proposed method does not require *tanδ, PI, DAR* information to operate. Hence measurement of these parameters using specialized costly equipment can be avoided.
5. The proposed method has been first tested using data collected from laboratory sample and thereafter using data obtained from real-life units. This emphasizes the capability of the proposed method to handle residual energy issues encountered in in-service units.

REFERENCES

[1] S. Chatterjee, S. Dalai, S. Chakravorti and B. Chatterjee, "Accelerating moisture content sensing of oil-impregnated paper insulation using frequency modulated square wave excitations", *IEEE Sensors Lett.*, vol. 3, no. 7, Jul. 2019.

[2] S. Chatterjee, A. K. Pradhan, S. Dalai, S. Chakravorti and B. Chatterjee, "A non-linear model for sensing moisture content in transformers at reduced time", *IEEE Sensors J.*, vol. 19, no. 12, pp. 4639-4646, Jun. 2019

[3] T. K. Saha, “Review of modern diagnostic techniques for assessing insulation condition in aged transformers”, *IEEE Trans. Dielectr. Electr. Insul.*, Vol. 10, pp. 903-917, 2003.

[4] C. Zachariades, R. Shuttleworth, R. Giussani and R. MacKinlay, "Optimization of a high-frequency current transformer sensor for partial discharge detection using finite-element analysis", *IEEE Sensors J.*, vol. 16, no. 20, pp. 7526-7533, Oct. 2016.

[5] M. Badar, P. Lu, Q. Wang, T. Boyer, K. P. Chen and P. R. Ohodnicki, "Real-time optical fiber-based distributed temperature monitoring of insulation oil-immersed commercial distribution power transformer", *IEEE Sensors J.*, vol. 21, no. 3, pp. 3013-3019, Feb. 2021.

[6] C. M. Banerjee, A. Baral and S. Chakravorti, "Detrapped Charge-Affected Depolarization-Current Estimation Using Short-Duration Dielectric Response for Diagnosis of Transformer Insulation," *IEEE Trans. Instrum. Meas.*, vol. 69, no. 10, pp. 7695-7702, Oct. 2020.

[7] T.K. Saha, P. Purkait and F. Müller, "Deriving an Equivalent Circuit of Transformers Insulation for Understanding the Dielectric Response Measurements", *IEEE Trans. Power Del.*, Vol. 20, No. 1,pp 149-157, 2005.

[8] A. Baral and S. Chakravorti, “Condition Assessment of Cellulosic Part in Power Transformer Insulation using Transfer Function Zero of Modified Debye Model”, *IEEE Trans. Dielectr. Electr. Insul.*, Vol. 21, No. 5, pp. 2028-2036, 2014.

[9] C. M. Banerjee, A. Baral and S. Chakravorti, "Influence of De-Trapped Charge Polarity in Sensing Health of Power Transformer Insulation," in *IEEE Sensors J.*, vol. 22, no. 7, pp. 6706-6716, 1 April1, 2022.

[10] D. Mishra, A. Baral, S. Chakravorti, "Compensating the Effect of Residual Dipole Energy on Dielectric Response for Effective Diagnosis of Power Transformer Insulation", *IET Sci. Meas .Technol.*, Vol. 12, No.3, pp 314-322,2018

[11] C. M. Banerjee, A. Baral, and S. Chakravorti, “Effective analysis of time-domain dielectric response for reliable diagnosis of power transformer insulation using statistical parameter evaluated from time varying model,” *IET Sci. Meas .Technol*, vol. 14, no. 1, pp. 48–55, Jan. 2020.

[12] C.M. Banerjee, S. Dutta, A. Baral and S. Chakravorti, "Influence of Charging Voltage Magnitude on Time Domain Dielectric Response of Oil-paper Insulation", *IET Sci. Meas .Technol.*, vol. 13, no. 6, Aug 2019.

[13] A. Garg, C. M. Banerjee, A. Baral and S. Chakravorti, "Diagnosis of Oil Paper Sample Using Capacitance Profile of Time Varying Model," Proc. 5th Int. Conf. Cond. Assesmt. Tech. Electr. Sys.(CATCON), Kozhikode, India, 2021, pp. 058-061.

[14] D. Mishra, A. K. Pradhan, A. Baral and S. Chakravorti, "Reduction of time domain insulation response measurement duration for fast and effective diagnosis of power transformer," *IEEE Trans. Dielectr. Electr. Insul.*, vol. 25, no. 5, pp. 1932-1940, Oct. 2018.

[15] IDAX300/350 - Insulation diagnostic analyzer", Jun. 2021, [online] Available: https://us.megger.com/insulation-diagnostic-analyzer-idax-series#overview.

[16] omicronenergy.com. 2022. “DIRANA-Brochure-ENU,” Accessed: Mar. 9, 2022. [Online]. Available: https://www.omicronenergy.com/download/document.

[17] D. Mishra, A. Baral and S. Chakravorti, "Denoising of time domain spectroscopy data for reliable assessment of power transformer insulation," *IET Gener. Transm. Distrib.*, vol. 14, no 8, pp.1500-1507, 2020.

[18] H. C. Verma, A. Baral, A. K. Pradhan and S. Chakravorti, "A method to estimate activation energy of power transformer insulation using time domain spectroscopy data," in *IEEE Trans. Dielectr. Electr. Insul.*, vol. 24, no. 5, pp. 3245-3253, Oct. 2017.

[19] Making Precision Low Current and High Resistance Measurements, Jan. 2022, [online] Available: https://download.tek.com/document/LowCurrentHiResistance_EHandbook.pdf.